Journal of Catalysis **211,** 226–234 (2002)
doi:10.1006/jcat.2002.3704

Propane Oxidation on Mo–V–Sb–Nb Mixed-Oxide Catalysts

1. Kinetic and Mechanistic Studies

Ekaterina K. Novakova, Jacques C. Védrine,[1] and Eric G. Derouane

Leverhulme Centre for Innovative Catalysis, Department of Chemistry, The University of Liverpool, Oxford Street, Liverpool L69 7ZD, United Kingdom

Received March 25, 2002; revised May 30, 2002; accepted May 30, 2002

Kinetic and mechanistic investigations were made of propane oxidation to acrylic acid over $Mo_1V_{0.3}Sb_{0.25}Nb_{0.08}O_n$ catalyst, calcined at 600°C in air, and activated at 500°C in O_2/He. The kinetic study allowed determination of the orders of propane disappearance and major products formation, and also emphasised the crucial effect of water on the activation energies of propane and oxygen. Propane and independently propene oxidation at various contact times enabled us to differentiate primary from secondary products and to propose a reaction scheme with three pathways: two major pathways leading to acrylic and acetic acids and a minor pathway leading to propionic acid. It was shown that acetic acid is formed via a route bypassing propene as an intermediate.

Key Words: **propane; propene; oxidation; acrylic acid; kinetics; reaction pathways; Mo–V–Sb–Nb oxides.**

INTRODUCTION

The direct oxidation of propane to acrylic acid using molecular oxygen as an oxidant has recently attracted a lot of attention in both academia and industry, both for fundamental reasons, which concern the understanding of alkane activation and oxygen insertion, and for economical reasons, such as the high abundance of propane in natural gas and its lower price than propene. To date, the industrial production of acrylic acid involves a two-step process, which consists of the propene oxidation to acrolein over multicomponent Mo–Bi–Co–Fe-based oxide catalysts at 320–330°C followed by the oxidation of acrolein to acrylic acid over Mo–V-based oxide catalysts at 210–255°C with an overall yield of approximately 87% (1). Unfortunately, until now no catalyst system has been reported for the direct oxidation of propane that is active and selective enough to substitute the existing industrial process; this is mainly due to the higher reaction temperatures required for the activation of the paraffin, which results in the enhancement of total oxidation reactions.

The oxidation of propane takes place via several different reaction pathways, leading to the formation of many partial oxidation products such as propene, acrolein, acetone, acrylic, propionic, and acetic acids as well as carbon oxides and water (2, 3). The reaction is generally believed to proceed via Mars–van Krevelen mechanism (4) with incorporation of lattice oxygen to form the aforementioned products followed by catalyst reoxidation by molecular oxygen. The oxidation of propane to acrylic acid requires four lattice oxygen atoms, abstraction of four hydrogen atoms from the substrate, insertion of two oxygen atoms from the lattice, and transfer of eight electrons, i.e., a coordinated action of the active sites as well as balanced redox properties of the catalyst to complete the catalytic cycle.

This article deals with the reaction kinetics and mechanism of propane partial oxidation to acrylic acid on $Mo_1V_{0.3}Sb_{0.25}Nb_{0.08}O_n$ mixed-oxide catalysts, which have not been addressed thus far. Catalysts with Mo–V–Sb(Te)–Nb–O compositions are prominent materials for this reaction as demonstrated by many recent patents (5–8) and in the open literature (9–16). However, a large diversity of oxygenated products has been observed depending on both the calcination, activation temperatures, and atmospheres, and on the reaction conditions applied.

The remote control mechanism (17) and the Mars–van Krevelen (4) kinetic models normally are used to best describe the behaviour of this type of catalyst-reaction system, but the complicated mathematical expressions together with the very complex structure and composition of the catalyst used prevent their application to this study. The rates of reactants disappearance and products formation were derived from a reaction–chemical-engineering point of view for differential-type reactors (18).

It is shown in the literature that the reaction network and products distribution are very sensitive toward the

[1] To whom correspondence should be addressed. Fax: +44 151 794 3589. E-mail: vedrine@liv.ac.uk.

0021-9517/02 $35.00

catalyst used (19). Significant differences in the reaction pathways are observed when the reaction is carried out over V–P–O catalysts (20), Te–P/NiMoO catalysts (11), and Mo–V–Te–Nb–O catalysts (13). We report here the first investigation of the kinetics of propane and propene oxidation on Mo–V–Sb–Nb mixed-oxide catalyst.

EXPERIMENTAL AND METHODS

The catalyst was prepared according to the patent literature (6) by a co-precipitation method, which consisted of preparation of slurry containing the salts of four metals (Aldrich): ammonium molybdate, ammonium metavanadate, antimony trioxide, and niobium oxalate. Initially the ammonium metavanadate (6 g) was dissolved in 154 ml water by heating and stirring, followed by the addition of the antimony trioxide (5 g) and ammonium molybdate (30.2 g) to the metavanadate solution. The suspension was refluxed at 90°C for 12 h and after cooling to room temperature an aqueous solution of niobium oxalate (3.7 g in 103 ml water) was added. The obtained slurry was stirred vigorously for 30 min, then concentrated and dried at 120°C. The catalyst precursor (44 g yield) of chemical composition $Mo_1V_{0.3}Sb_{0.25}Nb_{0.08}O_n$ was calcined at 600°C under a flow of predried air (90 ml min^{-1}) for 2 h. The sample was further activated in the reactor prior to reaction at 500°C in a mixture of 20% O_2 in He (50 ml min^{-1}).

The catalyst was characterised using BET, XRD, H_2-TPR, and NH_3-TPD techniques. The XRD characterisation was carried out at room temperature using a D-5000 Siemens diffractometer with a Co anticathode. The reducibility measurements were conducted using a Micromeritics TPO/TPR 2900 apparatus by flowing H_2 (5%) in Ar (50 ml min^{-1}) at the temperature range between 200 and 1100°C (10°C min^{-1}). The NH_3-TPD characterisation was carried out with the same equipment in the temperature range 200–600°C under He flow after saturation of the sample with pure ammonia (50 ml min^{-1}) at 80°C. For quantitative determination of NH_3 desorbed from the surface of the analysed catalysts during the analysis, a calibration of the detector signal was done by performing a TPD in He up to 800°C on three NH_4-exchanged MFI zeolites with different Si/Al ratio and the amount of the desorbed ammonia was plotted vs. the calculated concentration of ammonia in the zeolite.

The reaction was carried out in a continuous-flow, fixed-bed microreactor, with a water-generation unit, where water was produced by hydrogen oxidation over a Pt/Al_2O_3 catalyst at room temperature and after which the feed, which consisted of propane, oxygen, water, and helium, was directed either toward the catalyst bed or bypassing it. The reactor tube was made of stainless steel (30-cm length, 1.1-cm i.d.) set vertically with a mesh incorporated in the tube to keep the catalyst always in the same position, i.e., in the isothermal part of the furnace. The catalyst, which was ground to a fine powder and diluted by SiC, was packed between two layers of quartz wool; the height of each layer was about 1 cm. High-boiling products (water, acetone, acrolein, acetic and acrylic acids) were condensed in a system of two successive cold traps at room temperature and the rest of the products (CO, CO_2, and propene) as well as unreacted feed were analysed directly by GC. The condensation of the products was carried out for a total of 4.5 h (3 samples at 1.5 h each) and analysed after the reaction. The GC analyses were performed with a Varian 3400CX chromatograph, using three columns: Haysep D and MolSieve 13X packed columns set in series, where the online detected products and water were analysed, and an FFAP capillary column, connected in parallel to the other two, to analyse the condensate and propane.

The kinetic studies were conducted by analysis of the products at low propane and oxygen conversions (<10%), which is required for operating the reactor in a differential mode. This was achieved by introducing small amounts of catalyst (0.2 g) diluted in SiC to a total volume of 1.1 ml and using high total flow rates (60 ml/min, GHSV = 3273 h^{-1}). Only one of the reactants was varied at the time and the rest were chosen to be in excess and outside the explosion limits for the mixture of propane and oxygen. The study of the kinetic dependence on propane was performed by varying the propane concentration between 2 and 6 vol% and maintaining the others as follows: 60 vol% O_2, 25 vol% H_2O balanced with He. For the oxygen dependence, the concentration was varied between 5 and 60 vol% (10 vol% C_3H_8, 25 vol% H_2O, He balance) and for the water dependence, the concentration was varied between 0 and 60 vol% (10 vol% C_3H_8, 20 vol% O_2, He balance). The effect of reactant concentration was studied at four different temperatures ranging between 380 and 440°C.

Propane and propene oxidation reactions were studied independently as a function of the total gas hourly space velocity (i.e., the total flow rate) in the range between 1500 and 6000 h^{-1} over 1 and 0.7 g of catalyst diluted with SiC to get a total catalytic bed volume of 1.2 ml for propane and propene oxidation experiments, respectively. The reactions were performed at 400°C using the following feed composition: 52 vol% C_3H_8 (C_3H_6), 13 vol% O_2, and 35 vol% H_2O. The extrapolation of the results to zero contact time was done by using polynomial and linear fitting functions.

For all experiments, the reactant conversion was calculated as the number of moles of C in all products assuming 100% carbon balance with respect to the number of moles of C introduced. The selectivity toward a product was taken as fraction of the moles of C in the product with respect to the total moles of C in all products. Moles of C were defined as number of moles mltiplied by the number of C atoms in the reactant/product.

RESULTS AND DISCUSSION

1. Kinetic Description of the Reaction

The kinetic parameters for the propane oxidation were determined by following the products formation as a function of propane, oxygen, and water concentrations under reaction conditions required for a differential operating regime (reactants conversion lower than 10% at any temperature used). The obtained products comprised propene, acetone, acrolein, acrylic and acetic acids, and carbon oxides. Due to the very low selectivities to acrolein and acetone (between 0.5 and 1.5 mol% C), the formation of these products was not further investigated in this kinetic study. A blank reaction (SiC only, 1.2 ml) was carried out prior to conducting the kinetic and mechanistic studies and did not show any activity, nor did homogenous combustion of propane occur, since the sample was placed between two layers of quartz wool.

An essential condition for successful kinetic measurements is to ensure that the reaction is free of mass and heat transfer limitations. The nitrogen adsorption and BET analysis show that the catalyst used possesses no mesoporosity and negligible microporosity, which reflects its low surface area ($6.9\ m^2\ g^{-1}$). Therefore, no internal mass transfer limitations were expected with this catalyst. A diagnostic test for external mass transfer limitations was performed by simultaneously varying the weight of catalyst and the total flow of feed to maintain the total weight hourl space velocity constant between experiments. No change in the reactant conversion occurred.

XRD characterisation indicated the presence of several crystalline phases together with an amorphous component (Fig. 1). The major phase was MoO_3, together with $VSbO_4$ and a phase of the type $(M_yMo_{1-y})_5O_{14}$, e.g., $(V_{0.07}Mo_{0.93})_5O_{14}$ and $Nb_{0.09}Mo_{0.91}O_{2.8}$. *In situ* activation did not lead to a change in the surface area or phase distribution of the catalyst. H_2-TPR experiments showed that this material reduced to a high extent at high temperatures. At catalytic reaction temperature, only 2% of the total reducible species underwent a reduction. NH_3-TPD characterisation showed that the catalyst was only weakly acidic with a pK_a value determined from the calibration value of 5.9 and a predominant presence of weak and medium acid sites.

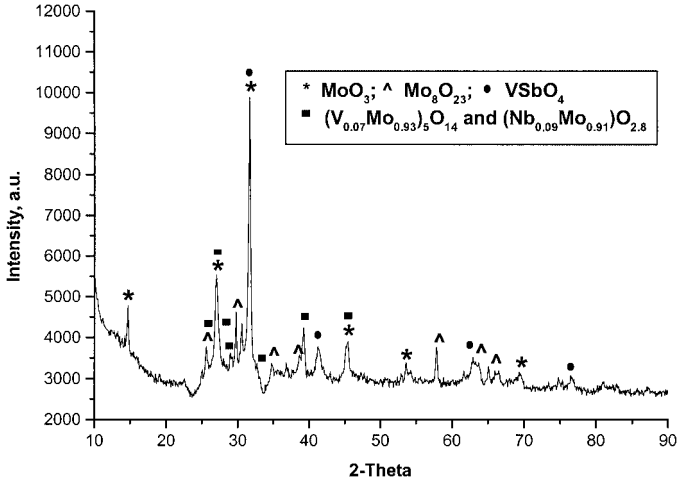

FIG. 1. XRD pattern of $Mo_1V_{0.3}Sb_{0.25}Nb_{0.08}O_n$ sample, calcined at 600°C under air and activated under 20% O_2/He at 500°C: MoO_3 (JCPDS: 35-0609), Mo_8O_{23} (05-0339), $VSbO_4$ (35-1485), $(V_{0.07}Mo_{0.93})_5O_{14}$ (31-1437), and $Nb_{0.09}Mo_{0.91}O_{2.8}$ (27-1310).

Propane disappearance is observed to be first order in propane at constant oxygen concentration and partial order in oxygen (0.26) at constant propane concentration. This is consistent with the reaction following the Mars–van Krevelen mechanism, becuase propane conversion is only partially dependent on the oxygen present in the feed. The rate constants (k), which were determined as the slope of propane disappearance vs. propane or oxygen concentration (Fig. 2), allowed the calculation of an apparent activation energy using the Arrhenius equation (Fig. 3). The relationship between $\ln\ k$ and $1/T$ is linear in the whole range of temperatures, which again confirms that no feed diffusion limitations occur. The Arrhenius parameters are calculated for both sets of rates of propane disappearance (with respect to propane and oxygen), which results in an apparent activation energy of 50 ± 1kJ mol^{-1} and a pre-exponential factor of 0.9 ± 0.1.

It is widely believed that propene is the only primary product of propane oxidation and, therefore, is directly dependent on propane concentration. This is confirmed by the first order of propene formation observed with respect to propane. However, the straight line does not pass through the origin of the graph (Fig. 2); its rate of appearance is zero at a propane concentration of 0.55 vol%. The reason for this is that the rate found experimentally for a product intermediate is the difference between the true rate of formation and the rate of product disappearance in the next step of the reaction. Thus, it is indicated that, at low propane concentration (<0.55 vol%), the propene formed is entirely converted to other products.

The dependence of propane oxidation to propene on the concentration of oxygen shows that there is a relationship between oxygen concentration and propene formation (Fig. 4), contrary to previous reports mentioning a zero order in oxygen (21, 22). In our case, a partial order of 0.26 is determined. Two explanations can be offered for the observed discrepancies. First, oxygen from the gas phase directly participates in the oxidative dehydrogenation of propane to propene. Second, the rate of reoxidation of the active sites on which the oxidative dehydrogenation occurs is slower than the propane transformation and is therefore dependent on oxygen concentration.

Considering the principle of the Mars–van Krevelen mechanism, the first explanation is not likely to apply except

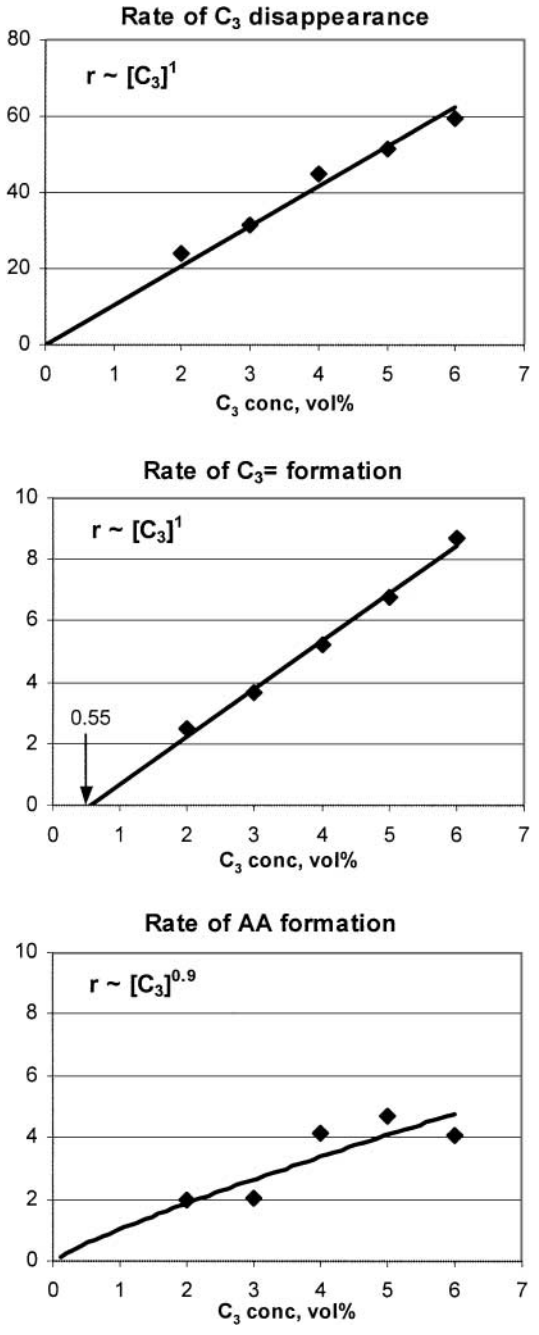

FIG. 2. Rates of propane disappearance and propene and acrylic acid formations ($\times 10^{-5}$ mol h^{-1} g^{-1}) with respect to propane concentration.

in the case of gas-phase reaction, but we demonstrated that the homogeneous reaction contribution to the product distribution was negligible under these experimental conditions due to the relatively low reaction temperature.

Our second hypothesis contradicts the literature data (21), wherein it is suggested that the rate of replacement of lattice oxygen by gaseous oxygen is a rapid process compared to its removal rate (hydrocarbon oxidation) and, therefore, the concentration of lattice oxygen at the catalyst surface is essentially constant and independent of the oxygen concentration in the gas phase (zero order). This is due to the different chemical/physical properties of Mo–V–Sb–Nb mixed oxide compared to the Ni–Mo–O studied therein.

To verify the validity of this explanation, the apparent activation energy for oxygen disappearance was calculated and found to be higher than that of propane disappearance (64 kJ mol^{-1}). It raises the question of possible attribution of the rate-determining step to oxygen activation and catalyst reoxidation under these reaction conditions rather than to propane activation.

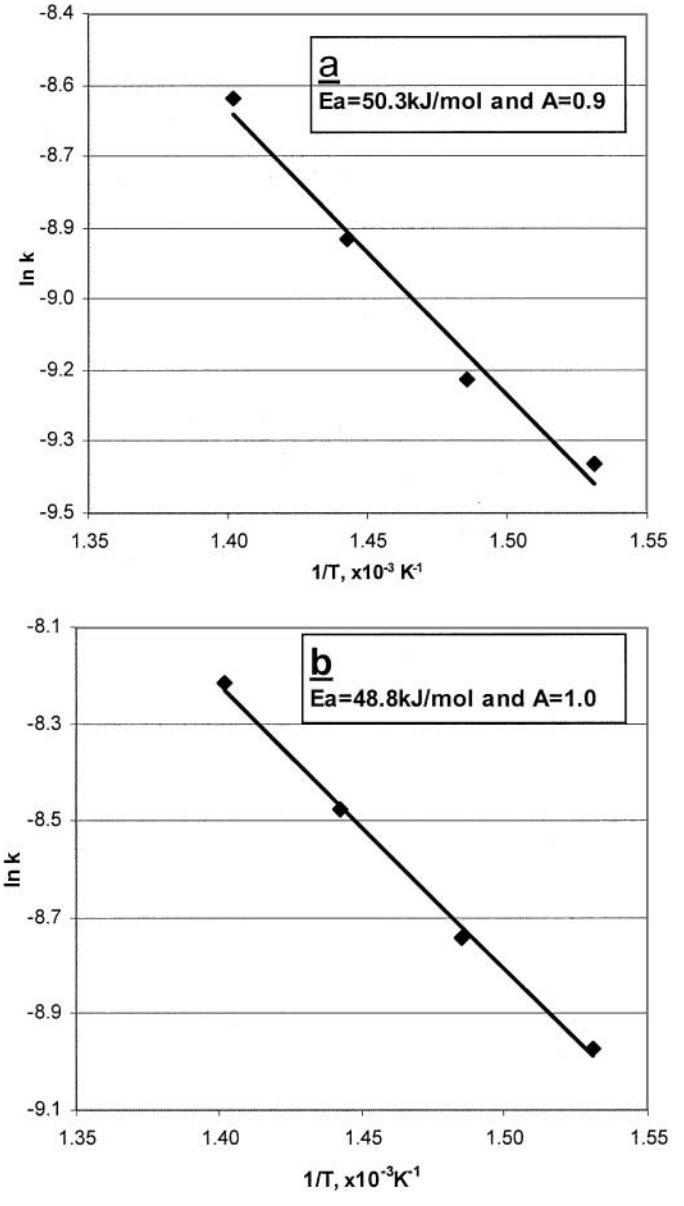

FIG. 3. Apparent activation energy (E_a) of propane with respect to (a) propane and (b) oxygen (A, pre-exponential factor).

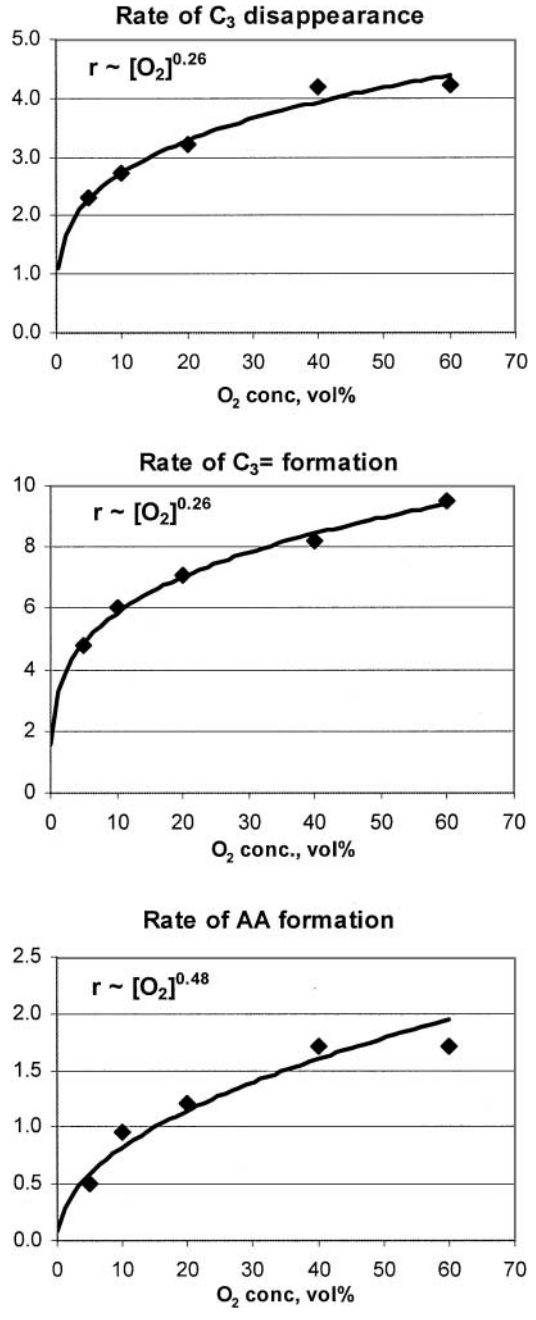

FIG. 4. Rates of propane disappearance and propene and acrylic acid formations ($\times 10^{-4}$ mol h^{-1} g^{-1}) with respect to oxygen concentration.

CO and CO_2 formations are first order in propane at all temperatures. CO_x can be formed at different stages of the reaction: (a) directly from propane or propene combustion at the catalyst surface or in gas phase, (b) simultaneously with acetic acid (C–C bond cleavage), or (c) overoxidation of acetic and acrylic acids.

The first order with respect to propane indicates that these are formed via surface-catalysed reaction and do not originate from a gas-phase reaction. The rate of CO_2 formation with respect to propane is found to be nearly constant with temperature with a rate constant of 2.8×10^{-5} mol h^{-1} g^{-1} (Fig. 5, dashed line). This implies that very small activation energy (1.2 kJ mol^{-1}) is required for the formation of CO_2 over this catalyst. The cause for the observed behaviour is not obvious; however, it suggests that CO_2 does not originate from a direct combustion of propane or overoxidation of acetic acid and acrylic acid, because the latter are temperature-controlled processes. Furthermore, the acetic acid formation with respect to propane is also found to be first order and the rate is found constant with temperature with a rate constant of 2.1 mol h^{-1} g^{-1} (Fig. 5, dashed line; $E_a = 1.3$ kJ mol^{-1}). The analogy between the kinetic behaviour of acetic acid and CO_2 formations indicates that they are probably formed simultaneously in the same stage of the propane oxidation process. In contrast, the rate of CO formation with respect to propane shows a strong dependence on temperature and, therefore, probably originates from the unselective propane oxidation.

The order of the CO_2 formation with respect to oxygen is found to be nearly one (1.1), the order of the CO formation is 0.8, and, in the case of acetic acid, the order is 0.5. Contrary to the results obtained from the dependence of propane on acetic acid and CO_2 formations, an oxygen-dependence study shows a certain relationship between the formation rate of these products and temperature (Fig. 5, solid line) with apparent activation energies for their formation of 34 and 30 kJ mol^{-1} for CO_2 and acetic acid respectively.

Acrylic acid formation is found to be close to first order in propane (0.9) and partial order in oxygen (0.48) as shown in Fig. 4. The observed deviations in the fitting function from the experimental data are due to the experimental difficulties in determining relatively low amounts of acrylic acid

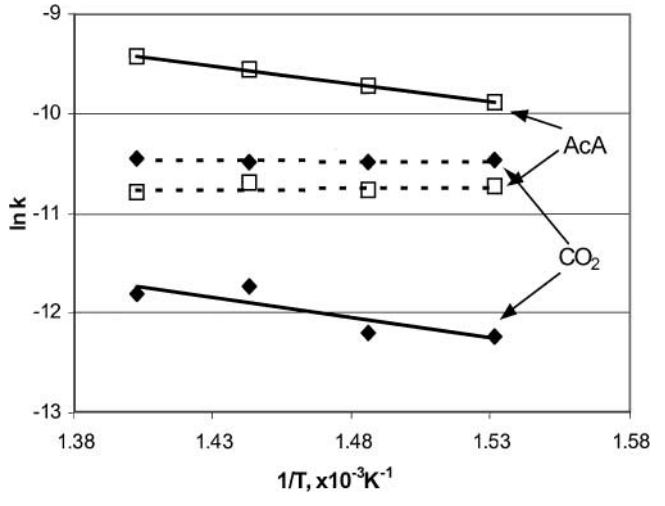

FIG. 5. Arrhenius plot of the temperature dependence of acetic acid (AcA) and CO_2 formations (dashed line, Arrhenius plot with respect to propane; solid line, with respect to oxygen).

TABLE 1

Apparent Activation Energy of Propane/Oxygen Disappearance under Water-Present (25 vol%) and Water-Free Conditions

Reactant	Activation energy (kJ mol^{-1})	
	$C_{H_2O} = 0$ vol%	$C_{H_2O} = 25$ vol%
Propane	68	50
Oxygen	64	64

(selectivities ranging between 2 and 12 mol% C). Contrary to what is found for acetic acid and CO_2, the rate of formation of acrylic acid with respect to propane is temperature dependent.

1.1. Effect of water concentration on the kinetics of propane oxidation. It was shown in the literature that water is an essential additive used to obtain higher propane conversion and selectivity toward oxygenated products (23–27). There are many speculations about how water affects the catalyst performance and product distribution, such as by facilitating oxygenates desorption from the catalyst surface (19, 23, 24), modifying the catalyst structure (25–27), and varying the rate of selected reactions (28). To clarify this point, kinetic measurements were conducted with water as the varied feed component.

The rates of propane and oxygen disappearance were calculated and plotted against the water concentration. Because the flow rates of propane and oxygen were maintained constant, the calculated rates depended only on the reactant conversion influenced by the amount of water present in the feed. In both cases, a zero order was obtained, confirming that water did not participate directly in propane transformation.

Apparent activation energies were calculated from the rates of propane/oxygen disappearance vs. temperature, with and without water present. It aimed at demonstrating whether water has an effect on the propane/oxygen activation either directly or by modifying the catalyst structure. The activation energies with/without water in the feed are summarised in Table 1.

The results clearly indicate that the presence of water in the feed decreases significantly the activation energy of propane but does not affect that of oxygen. The apparent activation energy of propane is slightly higher than that of oxygen under water-free conditions and, therefore, the rate-determining step is likely to be related to propane activation. Unfortunately, the reasons and the mechanism of the enhanced propane activation with water addition are not clear from our experiments. These results bring light to the question raised when determining propene formation. The experimental results suggested that the catalyst reoxidation was the rate-determining step, contrary to literature data. As mentioned before, Stern and Grasselli (21) found that under the conditions they used, hydrocarbon activation is the rate-determining step for propane oxidation. However, the experimental conditions used for their study did not include water in the feed: $C_3H_8(O_2) : O_2(C_3H_8) : N_2 = 6$–$42 : 25 : 69$–$33$ vol%. It is clear that for water-free conditions, there is no contradiction between the published data and our results.

2. *Mechanistic Investigations*

2.1. Propene oxidation. The determination of the reaction network on Mo–V–Sb–Nb mixed-oxide catalysts can be improved by independently studying propene and propane oxidation over the same catalyst and plotting the selectivity of the products formed against the contact time. The contact time varies in a range between 0.5 and 2.5 s; the microreactor used for this study did not allow contact times lower than 0.5 s, because of too-high turbulence in the reactants feed flow. However, it is possible to follow the sequence of the formation of the products by extrapolating their selectivity to zero contact time. Generally, primary products have nonzero intercept at zero contact time, whereas secondary or higher order products appear at a positive contact time. To obtain maximum information about the formation of the intermediate products, both propene and propane oxidations were performed at low conversions and under hydrocarbon-rich feed conditions (theoretical maximum conversion of 12.5%). This resulted in the formation of less total oxidation products, which are end products of the oxidation reactions.

Propene oxidation gives three products (acrolein, acetone, and acrylic acid) at 0-s contact time, but only the first two can be assigned to primary products because their selectivities decrease with contact time (Fig. 6). Acrylic acid progressively increases with contact time, which indicates

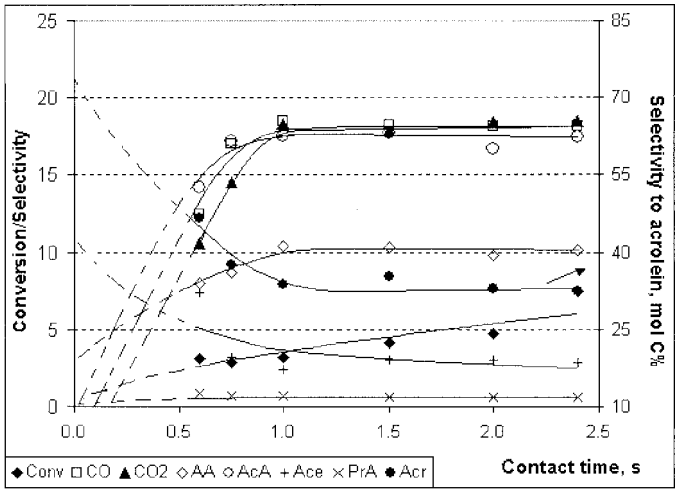

FIG. 6. Conversion/selectivity (mol% C) vs. contact time for propene oxidation with catalyst calcined in air (AA, acrylic acid; AcA, acetic acid, Acr, acrolein, Ace, acetone; and PrA, propionic acid).

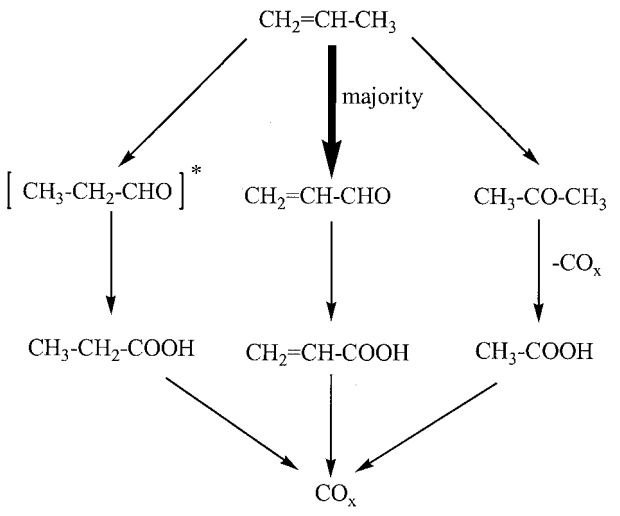

SCHEME 1. Proposed reaction pathways for propene oxidation over Mo–V–Sb–Nb mixed-oxide catalyst (∗, not detected).

that it is formed in the course of the reaction from another product, probably acrolein. The positive intercept with the ordinate suggests that propene is quickly transformed to the acid over this catalyst and even at very low contact time its amount is significant. Acetic acid and CO_x show behaviour of typical secondary products; the extrapolation shows an initial detection at positive contact time. Stationary formation of all products is reached at contact times larger than 1 s.

Propionic acid is formed in very small quantities (average selectivity of 0.7 mol% C). The extrapolation shows that its selectivity at 0-s contact time is practically zero. This means that propionic acid is a secondary product formed with propionaldehyde as intermediate, but the latter was not detected under these reaction conditions.

By accounting for the observed trends, it is possible to propose that in the case of propene oxidation on Mo–V–Sb–Nb mixed-oxide catalyst, the primary products are acrolein (majority) and acetone. These are oxidised to acrylic and acetic acids, which can be further transformed to CO_x. Additionally, propionic acid is formed. Therefore, a schematic reaction network can be proposed as represented in Scheme 1.

2.2. Propane oxidation. Considering the literature data (13, 29), we expected that propane oxidation experiments would bring evidence for the occurrence of propane oxidative dehydrogenation to propene as the sole first reaction step. But this appears not to be the case. Figure 7 shows the trend in propane conversion and products selectivity with contact time. Propane conversion steadily increases with contact time to a constant value of 9%

Three products are detected at contact time of zero seconds: propene, and acetic and acrylic acids. The shape of the trends suggests that propene and acetic acid are formed as primary products as their selectivity decreases with increase in contact time. The curve for propene selectivity decreases more rapidly, which indicates that it is a key intermediate that is quickly consumed in the next steps of the reaction. The acetic acid curve also declines with contact time, but at a much slower rate, and at contact times greater than 1 s it nearly reaches a plateau. This implies that it is partially converted to secondary oxidation products, but to a lesser extent. From these two trends, two options exist for acetic acid formation:

1. It is formed directly from propane without necessity for a propene intermediate.
2. It is formed from propene, which has a high rate of oxidation to acetic acid.

The second option is not very likely, because in this case acetone should also be formed as an intermediate of propene oxidation and should be detected at low contact time, which is not the case. Therefore, the idea of a route bypassing propene as intermediate should be adopted. This is supported by the mechanism proposed by Lin *et al.* (13), where isopropanol was suggested to be the intermediate leading to acetic acid. It was speculated that at high temperatures, isopropanol and acetone are highly reactive and exist only as surface-adsorbed species.

Acrylic acid and CO_x again exhibit behaviour of secondary products, even though the extrapolation suggests that they should be detected at contact times close to zero.

2.3. Reaction networks for propane and propene oxidation over Mo–V–Sb–Nb mixed-oxide catalysts. From our study a reaction scheme can be proposed (Scheme 2) for propane oxidation on Mo–V–Sb–Nb mixed-oxide catalyst, calcined at 600°C in air and activated in O_2/He, involving three main reaction pathways which leads to the

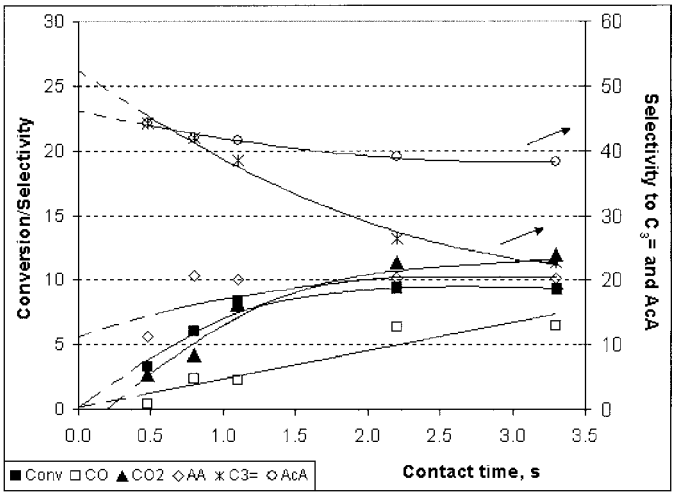

FIG. 7. Conversion/selectivity (mol% C) vs. contact time for propane oxidation with catalyst calcined in air (abbreviations as in Fig. 6).

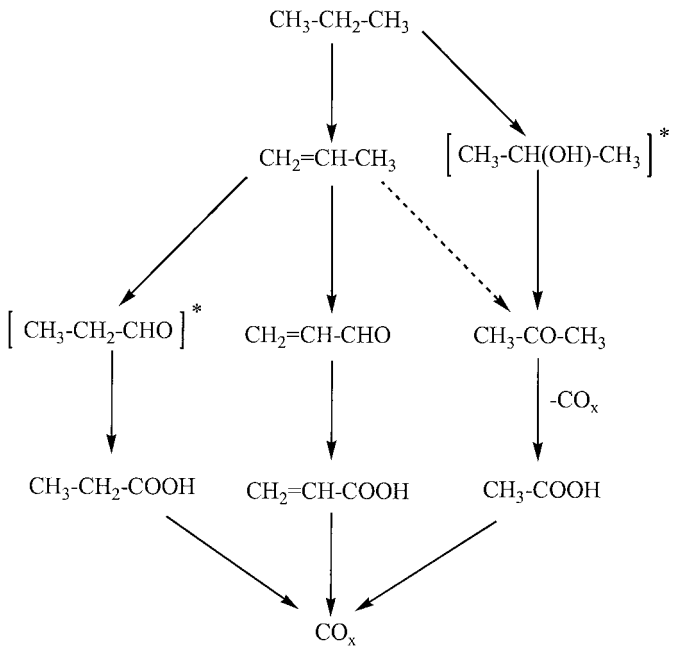

SCHEME 2. Proposed reaction pathways for propane oxidation over Mo–V–Sb–Nb mixed oxide catalysts (∗, not detected).

following:

- acrylic acid via formation of propene and acrolein. The latter product is not detected with propane oxidation experiments, indicating that it is highly reactive and quickly transforms into the corresponding acid as demonstrated in the propene oxidation experiments.
- acetic acid which shows behaviour of a primary product in the propane oxidation reaction and of a secondary product in the propene oxidation. Thus, in propane oxidation, acetic acid is formed mainly via a route which bypasses propene (probably via isopropanol) and only a fraction of it is formed via propene. This is supported by the twice-higher selectivity with propane oxidation.
- propionic acid, low amounts of which are detected in the propene oxidation reactions, but the necessary intermediates are not detected.

CONCLUSIONS

The Mo–V–Sb–Nb mixed-oxide catalyst used in this study was shown to be a mixture of an amorphous material and several crystalline phases, in particular MoO_3, $VSbO_4$, and $(M_yMo_{1-y})_5O_{14}$ with M = V ($y = 0.09$) and/or Nb ($y = 0.07$).

The kinetic studies provide information about the rates of reactant disappearance, rates of product formation, and their respective apparent orders. Unfortunately, due to the complexity of the reaction mechanism and of the catalyst composition, none of the classical mechanistic models, Mars–van Krevelen (4), Langmuir–Hinshelwood, or remote control (17), could be applied. However, although a precise picture could thus not be drawn, several interesting aspects were demonstrated. It was shown that the presence of water in the reaction significantly modifies the kinetic behaviour of the system reactants/catalyst by decreasing the activation energy of propane by approximately 25%. Under the experimental conditions (25 vol% H_2O) and temperature range 380–440°C, the reoxidation of the catalyst by molecular oxygen appears to be the rate-determining step.

Based on the results for propane oxidations over the catalyst, some aspects of the mechanism of the propane oxidation reaction become apparent:

1. The propene oxidation study identifies acrolein as a major primary product and acrylic acid as a secondary product, indicative of a pathway to acrylic acid via acrolein.
2. The propane oxidation study proved that propene is a major primary product, which further transforms to acrylic acid. Therefore, it can be concluded that acrylic acid is formed mainly via propene and acrolein intermediates.
3. Propene oxidation leads to the formation of acetic acid via acetone as a primary product. The propane oxidation study suggests that acetic acid is formed from propene as a primary product via acetone as mentioned previously or via an isopropanol intermediate to acetone and then acetic acid. The isopropanol intermediate was not detected during the experiments.
4. The kinetic results suggest that the side product formed in the course of acetone oxidation to acetic acid is CO_2, whereas CO is formed from overoxidation and/or combustion reactions.
5. Finally, traces of propionic acid are detected in the propene oxidation reactions.

REFERENCES

1. Idol, Jr., J. D., Standard Oil Corporation, U.S. Patent No. 2,904,580 (1959); Voge, H. H., and Adams, C. R., *Adv. Catal.* **17**, 151 (1967).
2. Bettahar, M. M., Costentin, G., Savary, L., and Lavalley, J. C., *Appl. Catal., A* **145**, 1 (1996).
3. Centi, G., Cavani, F., and Trifirò, F., *in* "Selective Oxidation by Heterogeneous Catalysis," p. 434. Kluwer Academic/Plenum, New York, 2001.
4. Mars, P., and van Krevelen, D. W., *Chem. Eng. Sci. Suppl.* **3**, 41 (1954).
5. Mitsubishi Chemical Corporation, JP 10045664-A (1996).
6. Toa Gosei Chem. Ind. Ltd., JP10137585-A (1996).
7. Lin, M., and Linsen, M. W., Rohm and Haas, EP0962253-A3 (1999).
8. Takahashi, M., Tu, X., Hirose, T., and Ishii, M., Toa Gosei Chem. Ind. Ltd., U.S. Patent No. 5,994,580 (1999).
9. Kim, Y.-C., Ueda, W., and Moro-oka, Y., *Appl. Catal.* **70**, 175 (1991).
10. Ushikubo, T., Oshima, K., Kayou, A., and Hatano, M., *Stud. Surf. Sci. Catal.* **112**, 473 (1997).
11. Kaddouri, A. C., Mazzocchia, C., and Tempesti, E., *Appl. Catal., A* **180**, 271 (1999).
12. Watanabe, H., and Koyasu, Y., *Appl. Catal., A* **194–195**, 479 (2000).
13. Lin, M., Desai, T. B., Kaiser, F. W., and Klugherz, P. D., *Catal. Today* **61**, 223 (2000).
14. Ueda, W., and Oshihara, K., *Appl. Catal., A* **200**, 135 (2000).

15. Holmes, S. A., Al-Saeedi, J., Guliants, V. V., Boolchand, P., Georgiev, D., Hackler, U., and Sobkow, E., *Catal. Today* **67**, 403 (2001).
16. Botella, P., Solsona, B., Martinez-Arias, A., and López Nieto, J. M., *Catal. Lett.* **74**, 149 (2001).
17. Weng, L. T., Ruiz, P., and Delmon, B., *Stud. Surf. Sci. Catal.* **72**, 399 (1991); Weng, L. T., and Delmon, B., *Appl. Catal., A* **81**, 141 (1992); Vande Putte, D., Hoornaerts, S., Tryrion, F. C., Ruiz, P., and Delmon, B., *Catal. Today* **32**, 255 (1996).
18. Levenspiel, O., "Chemical Reaction Engineering," 3rd ed., Wiley, New York, 1999.
19. Lin, M., *Appl. Catal., A* **207**, 1 (2001).
20. Ai, M., *J. Catal.* **101**, 389 (1986).
21. Stern, D., and Grasselli, R. K., *J. Catal.* **167**, 560 (1997).
22. Catani, R., Centi, G., Trifiró, F., and Grasselli, R. K., *Ind. Eng. Chem. Res.* **31**, 107 (1992).
23. Ai, M., *Catal. Today* **42**, 297 (1998).
24. Barrault, J., Batiot, C., Magaud, L., and Ganne, M., *Stud. Surf. Sci. Catal.* **110**, 375 (1997).
25. Volta, J. C., *Catal. Today* **32**, 29 (1996).
26. Rouzies, D., Millet, J. M. M., Siew Hew Sam, D., Volta, J. C., and Védrine, J. C., *Appl. Catal., A* **124**, 189 (1995).
27. Védrine, J. C., Millet, J. M. M., and Volta, J. C., *Catal. Today* **32**, 115 (1996).
28. Novakova, E. K., Ph.D. thesis, Department of Chemistry, Liverpool University, 2002.
29. Luo, L., Labinger, J. A., and Davis, M. E., *J. Catal.* **200**, 222 (2001).